A square planar gold(iii) bis-(1,1'-dimethyl-3,3'-methylene-diimidazol-2,2'-diylidene) trication as an efficient and selective receptor towards halogen anions: the cooperative effect of AuX and XHC interactions

Dalton Transactions

Accepted Manuscript

This article can be cited before page numbers have been issued, to do this please use: M. Baron, A. Dall'Anese, C. Tubaro, L. Orian, V. Di Marco, S. Bogialli, C. Graiff and M. Basato, *Dalton Trans.*, 2017, DOI: 10.1039/C7DT03672H.

This is an Accepted Manuscript, which has been through the Royal Society of Chemistry peer review process and has been accepted for publication.

Accepted Manuscripts are published online shortly after acceptance, before technical editing, formatting and proof reading. Using this free service, authors can make their results available to the community, in citable form, before we publish the edited article. We will replace this Accepted Manuscript with the edited and formatted Advance Article as soon as it is available.

You can find more information about Accepted Manuscripts in the author guidelines.

Please note that technical editing may introduce minor changes to the text and/or graphics, which may alter content. The journal's standard Terms & Conditions and the ethical guidelines, outlined in our author and reviewer resource centre, still apply. In no event shall the Royal Society of Chemistry be held responsible for any errors or omissions in this Accepted Manuscript or any consequences arising from the use of any information it contains.

ROYAL SOCIETY OF CHEMISTRY

rsc.li/dalton

View Article Online
DOI: 10.1039/C7DT03672H

Journal Name

ARTICLE

Square Planar Gold(III) bis-(1,1'-dimethyl-3,3'-methylene-diimidazol-2,2'-diylidene) Trication as Efficient and Selective Receptor Towards Halogen Anions: Cooperative Effect of Au···X and X···HC Interactions

Received 00th January 20xx,
Accepted 00th January 20xx

DOI: 10.1039/x0xx00000x

www.rsc.org/

Marco Baron,[a] Anna Dall'Anese,[a] Cristina Tubaro,[a,*] Laura Orian,[a] Valerio Di Marco,[a] Sara Bogialli,[a] Claudia Graiff,[b] Marino Basato[a]

Treatment of the tricationic gold(III) $[Au(MeImCH_2ImMe)_2](PF_6)_3$ complex **1-3PF$_6$** (Im = imidazol-2-ylidene) with excess halides affords complexes **1-3X** (X = Cl, Br, I), resulting from counter anion PF_6^-/X^- exchange. The ^{1}H chemical shift of the CH_3 groups and particularly of the CH_2 linker in DMSO-d_6 are different in the three complexes, thus suggesting selective X···HC interactions. Complex $\mathbf{1}^{3+}$ can be therefore used as halide sensor in DMSO and water. The host-guest interaction between the tricationic gold(III) complex and the halides Cl^-, Br^- and I^- in solution and in the solid state has been investigated by means of NMR titration experiments, DFT calculations and X-ray structure analysis. The electrostatic interaction between the halides and the triple formal positive charge on the metal centre, together with the CH···X hydrogen bonding between NHC ligand and halides contributes to forming stable supramolecular aggregates in solution and in the solid state. The complexing properties of $\mathbf{1}^{3+}$ are strongly influenced by the nature of the solvent. Formation of the 1:1 and 1:2 species ($\mathbf{1X}^{2+}$ and $\mathbf{1X_2}^{+}$) is observed in DMSO-d_6, while only the 1:1 aggregates ($\mathbf{1X}^{2+}$) are observed in D_2O (X = Cl, Br, I). Moreover, the selectivity towards the various halides is reversed in the two solvents, being in the order $Cl^->Br^->I^-$ in DMSO-d_6 and $I^->Br^->Cl^-$ in D_2O. The formation constants of the species $\mathbf{1X}^{2+}$ and $\mathbf{1X_2}^{+}$ in DMSO and $\mathbf{1X}^{2+}$ in water have been determined by fitting the NMR titration curves.

Introduction

Gold complexes with N-heterocyclic carbene (NHC) ligands have a broad range of applications which nowadays include homogeneous catalysis,[1] luminescent materials[2-4] and medicinal chemistry.[5] Furthermore, using NHCs ligands it is possible to synthesize stable gold complexes in high oxidation states (II+ and III+).[6,7]

We have recently reported on the straightforward synthesis of stable tricationic gold(III) complexes by transmetalation of silver carbene complexes with $KAuBr_4$ in mild conditions.[8] The obtained $[Au(MeImCH_2ImMe)_2]^{3+}$ (Im = imidazol-2-ylidene) tetra-NHC cation $\mathbf{1}^{3+}$ (Chart 1, a)) interacts with Br^- or silver bromides to afford in the solid state gold(III) centres with a distorted octahedral geometry. Most interesting, this strong axial electrostatic interaction between the square planar gold(III) cation and the halides is maintained in DMSO solution as recently reported also by Baker *et al.* (Chart 1, b).[9]

These findings prompted us to investigate the use of the tetra-NHC cation $\mathbf{1}^{3+}$ as halides sensor in solution. The anion receptors chemistry is a very active and important research field,[10] which covers, for example, sensing, extraction, transport, catalysis, self-assembling, and applications spanning from treatment of industrial waste to anion transport processes in the human body.[11]

Nowadays the application of organometallic complexes as anion sensors is very limited.[12] However, the tetra-NHC cation $\mathbf{1}^{3+}$ likely presents the right features for behaving as efficient sensor: i) high stability due to the presence of four NHC donors bonded to the gold(III) complex; ii) square planar coordination, which ensures an easy accessibility for the anionic substrates to the metal centre which, with its formal triple positive charge, is the core of the sensor; iii) water solubility, fundamental in environmental and biological studies.

[a] Dipartimento di Scienze Chimiche, Università degli Studi di Padova, via Marzolo 1, 35131 Padova, Italy.
[b] Dipartimento di Scienze Chimiche, della Vita e della Sostenibilità Ambientale, Università degli Studi di Parma, Parco Area delle Scienze 17/A, 43124 Parma, Italy.

Electronic Supplementary Information (ESI) available: ^{1}H and ^{13}C NMR spectra of complexes, titration experiments, Job Plots, computational details, crystallographic details, Cartesian coordinates for the computed species. See DOI: 10.1039/x0xx00000x

View Article Online
DOI: 10.1039/C7DT03672H

Chart 1. *Pseudo-octahedral* gold(III) NHC complexes reported by us (a)[8] and Baker (b).[9]

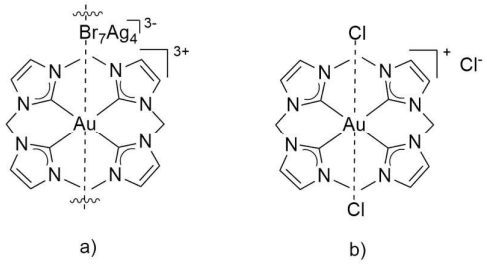

In this paper, we report on the application of $\mathbf{1}^{3+}$ as halides (Cl^-, Br^- and I^-) sensor in DMSO and in D_2O. We also examined in detail the interaction between the gold(III) complex and the halides by means of NMR spectroscopy, DFT calculations and X-ray single crystal analysis. Notably, from the analyses it emerges that the interaction between the gold(III) complex and the halides is not purely electrostatic and involves Au···X and CH···X bonding.

RESULTS AND DISCUSSION

Synthesis of 1-3X complexes and use of 1-3PF$_6$ as halide sensor

We started by synthesizing and isolating the gold(III) NHC complex $\mathbf{1}^{3+}$ having the halides Cl^-, Br^- and I^- as counter anions. This was easily achieved by exchange of the PF_6^- anion in **1-3PF$_6$** in acetonitrile solution with an excess of R_4NX (X = Cl, Br, I) to afford the immediate precipitation of the white complex $[Au(MeImCH_2ImMe)_2]X_3$ (**1-3X**), in which the three PF_6^- anions have been replaced by three halides X^- (Scheme 1). The HRMS are in agreement with the proposed stoichiometry; in particular, they show the signals related to the gold(III) metal tricationic complex interacting with one or two halides (Figures S11-S19). The ^{1}H NMR spectra in DMSO-d$_6$ are similar to that of **1-3PF$_6$**, except for a significant chemical shift difference for one proton of the bridging CH_2 group (Figure 1). Complex **1-3Cl** was recently reported by Baker and co-workers with a different synthetic procedure, starting from $KAuCl_4$ and the diimidazolium dichloride salt in the presence of lithium acetate as base.[9]

Scheme 1. Synthesis of complexes **1-3X** (X = Cl, Br, I) by counter anion exchange.[a]

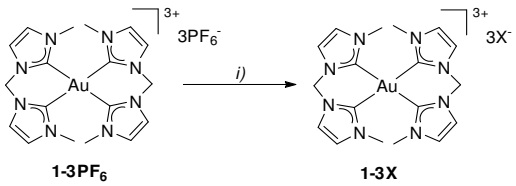

Reagents and conditions: $Et_4NCl{\cdot}H_2O$ (or Et_4NBr or $^nBu_4NI$) in CH_3CN (0.5 mmol in 10 mL), **1-3PF$_6$** in CH_3CN (0.05 mmol in 10 mL), rt, 1h.

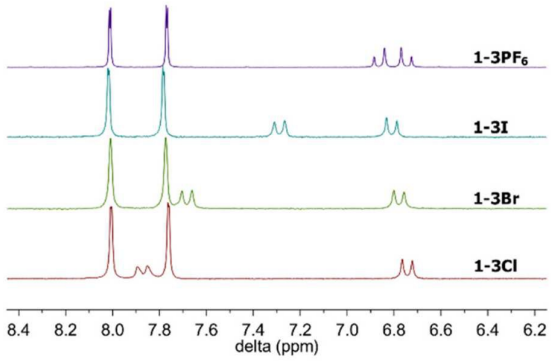

Figure 1. ^{1}H NMR spectra of complexes **1-3PF$_6$**, **1-3Cl**, **1-3Br** and **1-3I** in DMSO-d$_6$ in the region of the CH_2 protons of the bridge.

The difference in the signals of the methylene bridge in the NMR spectra of complexes **1-3X** (X = PF_6, Cl, Br, I) may be attributed to the interaction of the cationic NHC complex with the anions (Figure 2). The H_{exo} and H_{endo} protons of the methylene bridges experience a different chemical environment, pointing in opposite directions with respect to the gold-halogen position. Furthermore, the H_{endo}-H_{exo} exchange processes very slow in the NMR time scale: in fact, we have recently demonstrated with NMR spectra at different temperatures that for **1-PF$_6$** the AB system of the methylene bridge remains unchanged up to 150 °C in DMSO-d$_6$.[8] As a consequence, H_{exo} chemical shift is very similar for all the **1-3X** complexes while H_{endo} chemical shift strongly depends on the anion present in solution. Also the protons of the methyl wingtip groups are in proper position to interact with the anion (Figure 2). In this case however, the methyl groups are free to rotate and in the ^{1}H NMR spectrum, an averaged signal for the protons pointing to the anion and the other two pointing away is recorded.

We then performed NMR titration experiments, following the chemical shift of the H_{endo} protons in the ^{1}H NMR spectra upon addition of halide aliquots to a solution of **1-3PF$_6$** in DMSO-d$_6$ (Figure 3a and S20-S25).[‡] Figure 3b reports the δ values for H_{endo} signal against the concentration of the three investigated halides (Cl^-, Br^- and I^-).

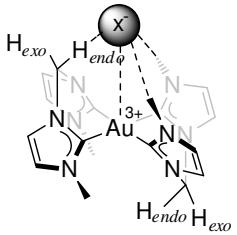

Figure 2. Representation of the molecular interactions in the complexes **1-3X**: Au···X, X···H_{endo} and X···HC_{CH3}.

View Article Online
DOI: 10.1039/C7DT03672H

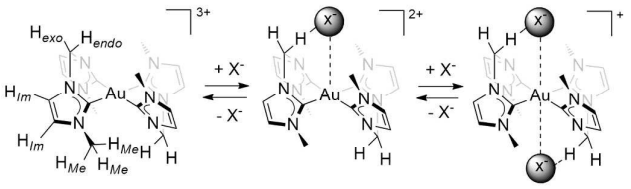

Scheme 2. Equilibria involving cation $\mathbf{1}^{3+}$ and halide ions. The protons of the ligand have been named in order to easily identify their signals in Figure 3.

Considering its molecular shape, complex $\mathbf{1}^{3+}$ has two identical sites for binding anions, with the possibility of forming 1:1 and 1:2 adducts (Scheme 2). The rate of conversion between these species is fast in the NMR time scale, so that a single averaged set of signals is observed.

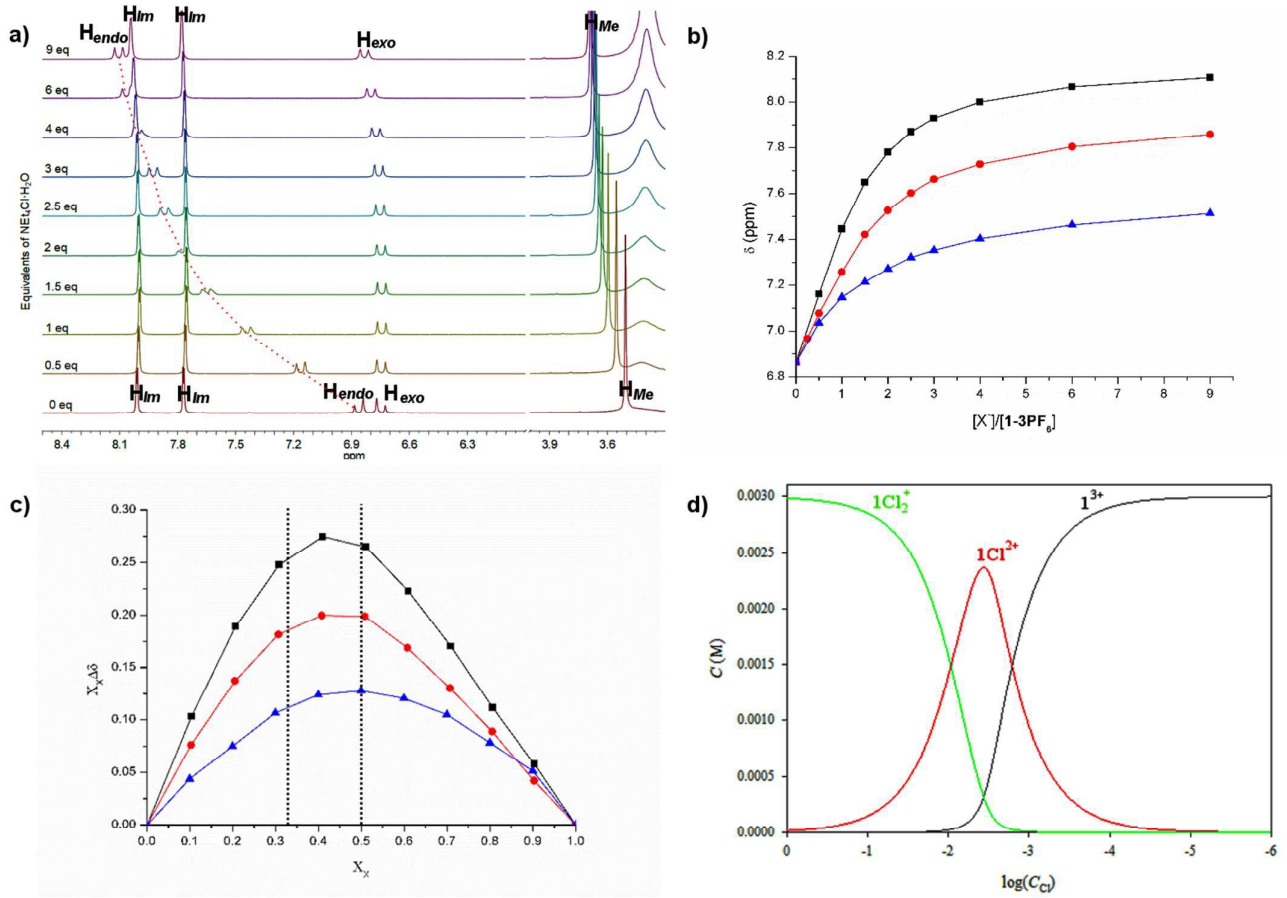

Figure 3. a) NMR titration of **1-3PF$_6$** (initial concentration 7.26 mM) with different amounts of chloride ions ($Et_4NCl·H_2O$) in DMSO-d_6. b) Variation of the chemical shift of the H_{endo} of the CH_2 bridge as a function of the added X^- (^{1}H NMR in DMSO-d_6): X=Cl^-, black line; X=Br^-, red line; X=I^-, blue line. c) Job plot in DMSO-d_6 for the interaction of $\mathbf{1}^{3+}$ and X^- ([**1-3PF$_6$** + X^-]= 5 mM): X=Cl^-, black line; X=Br^-, red line; X=I^-, blue line. d) Distribution curves for the complexes formed by treatment of $\mathbf{1}^{3+}$ with Cl^- in DMSO at a typical $\mathbf{1}^{3+}$ concentration (0.003 M).

Table 1. Stability constants (logβ) and chemical shift ($\Delta\delta$ of CH_2 protons, ppm, with reference to **1-3PF$_6$**) for $\mathbf{1X}^{2+}$ and $\mathbf{1X_2}^{+}$ complexes, as obtained from ^{1}H-NMR titrations and Job plots at 25 °C. logβ refers to the reaction $\mathbf{1}^{3+} + i\mathrm{X}^- = \mathbf{1X}_i^{(3-i)+}$ (i = 1 or 2).[a,b]

Solvent	Anion	$\log\beta_{\mathbf{1X}^{2+}}$	$\Delta\delta_{CH_2(\mathbf{1X}^{2+})}$	$\log\beta_{\mathbf{1X}_2^{+}}$	$\Delta\delta_{CH_2(\mathbf{1X}_2^{+})}$
DMSO	Cl	4.062 (0.093)	0.6153 (0.0053)	6.390 (0.097)	1.3029 (0.0035)
DMSO	Br	3.685 (0.074)	0.4368 (0.0047)	5.775 (0.075)	1.0969 (0.0011)
DMSO	I	2.552 (0.045)	0.488 (0.016)	3.876 (0.075)	0.847 (0.028)
H_2O	Cl	1.666 (0.021)	0.2843 (0.0068)	n.d.	n.d.
H_2O	Br	1.8694 (0.0089)	0.3959 (0.0032)	n.d.	n.d.
H_2O	I	2.156 (0.018)	0.4278 (0.0069)	n.d.	n.d.

[a] It is assumed that PF_6^-, albeit slightly interacting with the ligand, is not coordinated to the gold centre. In fact, addition of PF_6^- does not modify the ^{1}H NMR spectrum of **1-3PF$_6$** (see Figure S32). [b] Standard deviations for logβ and $\Delta\delta$ are reported in brackets.

View Article Online
DOI: 10.1039/C7DT03672H

In particular, the experimental data (NMR titrations and JOB plot experiments) were elaborated for each **1**-halide system by assuming different speciation models, which included the presence of the following complexes (taken alone or as mixtures): $\mathbf{1_2X^{5+}}$, $\mathbf{1X^{2+}}$, $\mathbf{1_2X_2^{4+}}$, $\mathbf{1X_2^{+}}$, $\mathbf{1X_3}$. The best fitting results (i.e. the lowest sum of squares) were obtained considering the presence of a mixture of 1:1 (complex $\mathbf{1X^{2+}}$) and 1:2 (complex $\mathbf{1X_2^{+}}$) host:halide species (Figures 3 and S20-S28). Data elaboration[13] allowed also to compute the stability constants and the chemical shifts of the complexes; the data obtained are reported in Table 1.

As an example, the distribution curves for the complexes formed by $\mathbf{1^{3+}}$ with Cl^- in DMSO at a typical $\mathbf{1^{3+}}$ concentration (0.003 M) used in these NMR experiments are reported in Figure 3d; distribution curves for Br^- and I^- are reported in the Supporting Information (Figures S30 and S31). According to these curves, the complexes start to form when the total halide concentration approximately exceeds 10^{-4} M, and all $\mathbf{1^{3+}}$ is completely bound when the total halide concentration exceeds 10^{-1} - 10^{-2} M. A covalent coordination of the halides to the metal cationic complex is limited by electronic reasons, considering the d^8 electronic configuration of gold(III) which stabilizes a square planar coordination geometry. Nonetheless, the high positive charge on the complex (3+) favours a strong mostly electrostatic interaction with the incoming halide to form the five and six-coordinated complexes $\mathbf{1X^{2+}}$ and $\mathbf{1X_2^{+}}$. These findings compare well with the structural and conductibility data on **[1Cl$_2$]Cl**.[9] We have observed, for **1-3Cl**, signals of the CH_2 bridging group at 6.74 and 7.87 ppm to be compared to those at 6.79 and 8.09 ppm for **[1Cl$_2$]Cl**. This may be justified assuming that some solvolysis occurs in our conditions and, as confirmed by the titration curves, further addition of Cl^- leads ultimately to the exclusive presence of $\mathbf{1Cl_2^{+}}$ in solution (chemical shifts identical to those reported for **[1Cl$_2$]Cl**).

These combined effects (high metal charge and X···HC interactions) justify the high values of the stability constants in DMSO (up to 4.062 and 6.390 for $\log\beta_{\mathbf{1Cl^{2+}}}$ and $\log\beta_{\mathbf{1Cl_2^{+}}}$ relative to chloride) and the decrease of the complex strength from Cl^- to Br^- ($\log\beta_{\mathbf{1Br^{2+}}}$ = 3.685) and I^- ($\log\beta_{\mathbf{1I^{2+}}}$ = 2.552). These values of $\log\beta$ can be compared to those found for organic anion receptors[14-16] based on polyimidazolium salts (Cl, 2.67; Br, 2.33 and I, 1.85;[16a] Cl, 4.27; Br, 4.21[17]) ammonium (Cl, 2.06[18]), polyamides (Cl, 3.47; Br, 1.60)[19].

Metal based receptors are less common[12] and normally may involve anion coordination, like in a zinc dinuclear complex based on pyrrole macrocylic ligands (Cl, $\log\beta$ 4.51 in DMF)[12f].

Turning to our gold based anion receptor, the second halide addition is less favoured (ca. 2 log units difference) compared to the first one, as expected for the X^- interaction with a less charged $\mathbf{1X^{2+}}$ complex.

Analogous experiments have been run also in deuterated water as solvent (Figures 4 and S32-S38), considering the increasing interest towards anion sensing in water.[10c,20] The stability constants are lower in water ($\log\beta_{\mathbf{1X^{2+}}}$ = 1.666 (Cl^-), 1.869 (Br^-) and 2.156 (I^-)) than in DMSO, as expected, due to a higher dielectric constant of the solvent and to its competition on the Au and CH electrophilic centres. Moreover, the order of stability constant in water is reversed, being higher for the iodide anion, and no evidence is found in the explored concentration range for the formation of $\mathbf{1X_2^{+}}$. Titration with HCl instead of $Et_4NCl{\cdot}H_2O$ does not show any significant variation in the distribution of products, indicating that the acceptor system is stable and very slightly affected by change of acidity in the pH range 1-7 (Figure 4). This is an interesting result as, in general, organic receptors are very sensitive to pH variation, being often protonated systems,[10c,14b] and working properly in buffered solvent.

Some insight on the factors influencing the observed behaviour can be derived from the analysis of the data in Table 1. The observed trend in DMSO appears to reflect mainly the electronegativity of the involved halogens, so that the highest formation constant is observed for Cl^-, which gives also the strongest interaction with one CH_2 hydrogen, as indicated by the highest values of induced chemical shift ($\Delta\delta_{CH2}$ 0.615 ppm for $\mathbf{1X^{+}}$ and 1.303 ppm for $\mathbf{1X_2^{+}}$).

The situation remarkably changes in water, where competition with solvent becomes very important. Water in fact may behave as an electrophile towards X^- weakening its interaction with the Au^{3+} and HC centres. This is confirmed by the lower values of the observed $\Delta\delta$ compared with DMSO. It is expected that water interacts better with Cl^- than with Br^- and I^-, following the order of the solvation energy. The net result is a greater stability constant for $\mathbf{1I^{2+}}$, i.e. the complex of the less solvated anion (iodide), which is also less sensitive to H_2O competition, giving the strongest X···HC interaction ($\Delta\delta_{CH2}$ 0.428 ppm).

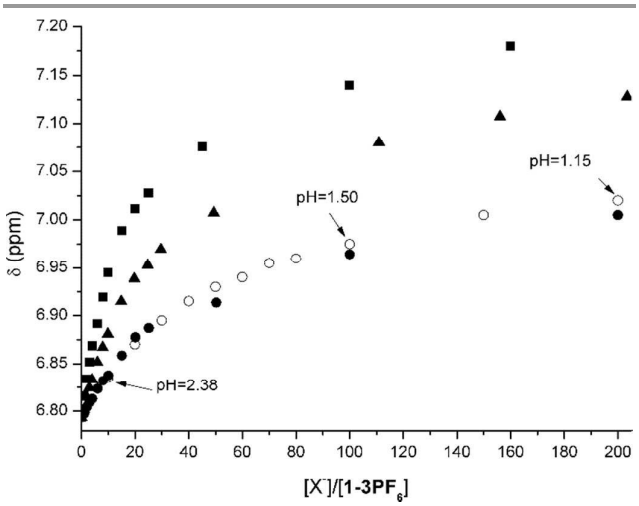

Figure 4. Chemical shift variation of the H_{endo} of the CH_2 bridge (^{1}H NMR in D_2O) as a function of the added halides: (●) titration with Et_4NCl; (○) titration with HCl; titration with Et_4NBr (▲); titration with Bu_4NI (■).

DFT calculations

The C_{2h} geometry of the isolated Au(III) complex has been recently calculated and reported by some of us, in nice agreement with the crystallographic parameters.[8] The frontier

View Article Online
DOI: 10.1039/C7DT03672H

molecular orbitals, i.e. the HOMO and the LUMO, which span the irreducible representations B_g and B_u, respectively, exhibit significant differences: the former is mainly ligand centred with a small contribution of Au d_{yz}, while the latter has a large Au p_y lobe.[8]

In order to gain insight into the nature of the interaction between the gold centre and one and two halide ion(s) X^-, the series of complexes **1Cl^{2+}**, **1Br^{2+}**, **1I^{2+}** and **1Cl$_2^+$**, **1Br$_2^+$** and **1I$_2^+$** were built and optimized under C_s symmetry constraint. Then, the bonding analysis was performed partitioning the molecules into two fragments, i.e. the **1^{3+}** complex and the halide(s); the results are shown in Table 2.

The **1X^{2+}** series is discussed first. The molecular structures with Cl and I are very similar to **1Br^{2+}**, recently reported by some of us.[8] A close proximity between the coordinated halogen atom and one proton of the methylene bridge oriented on the same side is evident; all distances are much shorter than the sum of the atomic Van der Waals radii, i.e. at 2.29 Å (Cl···H), 2.42 Å (Br···H) and 2.61 Å (I···H), respectively. Slightly larger separations, but also in this case much below 3.0 Å, are measured between a proton from each of the two methyl groups pointing toward the halogen and the halogen itself, i.e. 2.43 Å (Cl···H), 2.56 Å (Br···H) and 2.75 Å (I···H), respectively. These intramolecular interactions provide extra-stabilization to the complexes and influence the overall structure, as observed in other cases in combined crystallographic and computational studies.[21] The charge on the gold centre decreases with increasing halogen size, i.e. +0.3662, +0.3590 and +0.3494 for Cl, Br and I, respectively. The trends of ΔE values for the **1X^{2+}** complexes can be directly compared to the trend of the experimental $\beta_{\mathbf{1X}^{2+}}$ constants, being the gas-phase energies of the reactions reported in equation (1).

1^{3+} + X^- → **1X^{2+}** (1)

1^{3+} + 2X^- → **1X$_2^+$** (2)

They nicely match to the experimental trend found in DMSO, opposite to the trend found in the highly polar water. Important, upon increasing the halogen size, the halide coordination to the gold centre leads to an energetically less stabilized product.[§] From the analysis it appears that this is not ascribed to strain which remains almost constant, due only to the **1^{3+}** deformation, but rather to the interaction term, which decreases by 6.05 and 10.71 kcal mol^{-1} when going from chloride to bromide and iodide, respectively. From EDA, it emerges that the difference between chloride and bromide is due to the increase of Pauli repulsion with increasing halogen size by 7.71 kcal mol^{-1}, which is not compensated by the more stabilizing dispersion interaction contribution which increases (in absolute value) from -9.25 to -11.06 kcal mol^{-1}. In fact, no appreciable variation of the electrostatic and orbital interaction terms is computed. In contrast, when going from bromide to iodide, the larger dispersion contribution and the increase (in absolute value) of the orbital interaction compensate the increased Pauli repulsion. Nevertheless, the electrostatic term weakens by 4.91 kcal mol^{-1}, since the negative charge becomes more diffuse when going from bromide to iodide, thus accounting for the overall destabilization.

By inspecting the occupied frontier MOs one finds that in **1Cl^{2+}** and **1Br^{2+}** HOMO-2, HOMO-1 and HOMO are close in energy, spanning the irreps A', A'' and A', respectively (Table S13).

HOMO and HOMO-2 are a combination of p_x and p_y orbitals of the halide with a small contribution of the LUMO of the **1^{3+}**; this last MO is a combination of p_y atomic orbitals of the metal centre and of the imidazole N and C atoms.[8] HOMO-1 composition is dominated by the halide p_z orbital combined with the LUMO of **1^{3+}**. When going from Cl to Br and I the p filled halide orbitals are pushed to higher energy.

In HOMO and HOMO-1 of **1X^{2+}**, p_z and p_x contributions increase along the group. In contrast, in HOMO-2, the p_y percentage increases and in **1I^{2+}** it is shifted to a lower energy than HOMO and HOMO-1, due to combination also with LUMO+9 of the **1^{3+}** fragment which has almost 20% Au p_y character.

Moving to the **1X$_2^+$** series, for which the optimization was carried out imposing C_{2h} symmetry constraint, structural features similar to those commented for the **1X^{2+}** complexes are observed. For example, close proximity is evident between the halogen atom and the methylene and methyl protons pointing toward it. Distances are 2.23 and 2.43 Å, 2.37 and 2.54 Å, 2.57 and 2.71 Å for Cl, Br, and I derivatives, respectively.

Table 2. Energy decomposition analysis of the C_s optimized **1X^{2+}** complexes (X= Cl, Br, I) and of the C_{2h} optimized **1X$_2^+$** complexes (X= Cl, Br, I); all values are in kcal mol^{-1}; level of theory: ZORA-BLYP-D3(BJ)/TZ2P sc.

	1Cl^{2+}	**1Br^{2+}**	**1I^{2+}**		**1Cl$_2^+$**	**1Br$_2^+$**	**1I$_2^+$**
ΔV$_{elstat}$	-254.01	-253.78	-248.87	**ΔV$_{elstat}$**	-463.65	-457.02	-442.40
ΔE$_{Pauli}$	76.38	84.09	89.47	**ΔE$_{Pauli}$**	104.80	113.91	119.47
ΔE$_{oi}$	-50.28	-50.35	-53.39	**ΔE$_{oi}$**	-77.31	-74.89	-77.40
A'	*-38.60*	*-39.21*	*-42.60*	A_g	*-21.25*	*-19.78*	*-19.84*
A''	*-11.68*	*-11.14*	*-10.80*	A_u	*-12.15*	*-11.41*	*-10.98*
				B_g	*-12.09*	*-11.49*	*-11.23*
				B_u	*-31.81*	*-32.22*	*-35.35*
ΔE$_{disp}$	-9.25	-11.06	-13.66	**ΔE$_{disp}$**	-16.72	-19.83	-24.32
ΔE$_{int}$	-237.16	-231.11	-226.45	**ΔE$_{int}$**	-452.88	-437.83	-424.65
ΔE$_{strain}$	1.93	2.03	2.40	**ΔE$_{strain}$**	55.51	52.71	50.17
ΔE	-235.23	-229.08	-224.05	**ΔE**	-397.37	-385.12	-374.48

View Article Online
DOI: 10.1039/C7DT03672H

These findings fully justify the trend exerted by the halides in the chemical shift of the *endo* proton of the methylene bridge, and are in discrete agreement with solid state structures (see further in the text).

From the values of Table 2, one can notice that strain as well as interaction contribute to the total energy. The contribution to strain becomes larger in the doubly negative charged fragment formed by the two halides, decreasing from Cl to Br and I. It is worth to notice that the strain contribution due to the deformation of the $\mathbf{1}^{3+}$ fragment is almost constant, i.e. 2.97, 2.60 and 2.65 kcal mol^{-1}; in contrast, the strain contribution of the bis-halide fragment drops by 9.23 kcal mol^{-1} from Cl to I, and is thus responsible of the decrease of the total strain. The interaction decreases remarkably too, leading to an overall large destabilization of the $\mathbf{1X_2^+}$ complex when increasing halogen size, with energy changes being roughly twice those computed for the $\mathbf{1X^{2+}}$ analogues. From EDA, when going from Cl to Br, the only stabilizing term is the dispersion. The overall destabilization is 15.05 kcal mol^{-1}. Conversely, when going from Br to I, ΔE_{oi} becomes more negative by 2.51 kcal mol^{-1}. Despite additional 4.49 kcal mol^{-1} due to dispersion, the total interaction decreases by 13.18 kcal mol^{-1}. Also in this case, the charge on the gold centre decreases with increasing halogen size, i.e. +0.3875, +0.3776 and +0.3649 for Cl, Br and I, respectively.

The frontier molecular orbitals HOMOs of the Cl and Br complexes are mainly formed by the halides' p_y orbitals spanning the irreducible representation Σ_g and Au d_{x2-y2}/d_{z2}, while LUMOs have large contribution from the C and N p_y and a small percentage of Σ_u (p_y) of the halides. In the case of iodine, the HOMO composition is analogous, but the LUMO is formed by Au d_{xz} lobes and ligand p_x and p_z, without any contribution by the halides.

In order to rationalize the trends for the thermodynamic constants β, we have computed the energies of reactants and products of the reactions of equations (1) and (2) in the two different solvents, i.e. DMSO and water. Calculations have been done using the geometries optimized in gas-phase as well as re-optimizing the species in solvent, with and without symmetry constraint, but no appreciable difference was obtained in the structures and consequently in their energies (Table S14).

Focusing on the formation of $\mathbf{1X^{2+}}$, for which experimental data are available in both solvents, it is evident that the trend in water is well reproduced and is opposite to the trend in gas-phase. However, the $\beta_{\mathbf{1X^{2+}}}$ trend in DMSO is not recovered: calculated values suggest a more and more stabilized product with increasing halogen size. The solvent, treated in our model as a bulk dielectric medium, cannot have a molecular role in the reactions in DMSO: this was verified by performing some geometry optimizations which excluded the coordination of DMSO to the metal centre. This case was already discussed in literature[22] and, in agreement, our calculations do not predict coordination of DMSO to Au(III). Another hypothesis is that, at the employed level of theory, the energy of the solvated halide is overestimated in solvent, an error which decreases with increasing halogen size and increasing solvent polarity.[§§,23]

Crystallographic characterization

The simple PF_6^-/X^- exchange reaction employed in the syntheses of **1-3X** in acetonitrile quickly afforded very insoluble powders, thus, considering the importance of crystallographic evidences on Au···X and X···HC interactions, we decided to obtain and crystallize them in the presence of iodine in excess. The addition of iodine reduces the concentration of free halide through formation of polyhalogenic anions, thus preventing precipitation and allowing the obtainment of clear solutions. Moreover this procedure may be useful in testing the ability of the tricationic complex to stabilize new and extended counter anions (polyhalides in particular),[24] as already shown with the silver polybromides chain we reported in a previous work.[8] All syntheses involved the slow diffusion of diethyl ether into an acetonitrile solution of $\mathbf{1\text{-}3PF_6}$ and X^-/I_2 in approximate 1:30:40 molar ratio. The resulting microcrystalline precipitate as a rule contained few crystals suitable for X-ray analysis.

The crystal structure of the three compounds is characterised by the $[Au(MeImCH_2ImMe)_2]^{3+}$ tricationic unit, in which the gold atom shows a square planar environment with Au-C bond distances that are in good agreement with those found in $\mathbf{1\text{-}3PF_6}$ and in similar compounds.[8,9,25] The C1-Au-C2 bond angle, as expected, is slightly narrower than 90° as observed in $\mathbf{1\text{-}3PF_6}$. In Table 3, the most important bond distances and angles of the cationic complexes are reported, and compared to the analogous ones in $\mathbf{1\text{-}3PF_6}$.

In all the compounds, the two chelating ligands are disposed in opposite site with respect to the AuC_4 coordination plane. In compounds $\mathbf{1\text{-}Cl,2I_3}$ and $\mathbf{1\text{-}3Br^-I_2}$, this inversion is imposed by the crystallographic symmetry of the space group. The AuC_4 coordination is not deviated from planarity. The value of the dihedral angle between the imidazole rings (A and B) and the coordination plane AuC_4 is approximately the same and slightly smaller than the values observed in $\mathbf{1\text{-}3PF_6}$.

In the crystal packing of the compounds, two halogen atoms in the form of monoatomic anion (Cl and Br) in $\mathbf{1\text{-}Cl,2I_3}$ and $\mathbf{1\text{-}3Br^-I_2}$ respectively, or in the form of the terminal I atom of the I_3^- anions in $\mathbf{1\text{-}3I_3}$, occupy unusual additional axial coordination sites. The distorted octahedral coordination is rather rare for Au(III) complexes.[9] The Au···X distance is 3.169, 3.631 and 3.684 [4.018] Å for $\mathbf{1\text{-}Cl,2I_3}$ $\mathbf{1\text{-}3Br^-I_2}$ and $\mathbf{1\text{-}3I_3}$ respectively (3.148(2) and 3.192(2) Å for **1-3Cl**)[9]. Those distances are longer than Au-X covalent bonds, but are significantly shorter than the sum of the van der Waals radii of the atoms (4.14, 4.18 and 4.36 Å for Au-Cl, Au-Br and Au-I respectively).[26] Also in the crystal packing of compound $\mathbf{1\text{-}3PF_6}$,[8] F atoms of the PF_6^- anions occupy largely distorted axial octahedral coordination sites. The Au···F distance is 3.414 Å slightly shorter than the sum of the van der Waals radii which is 3.78 Å.

Considering the crystal packing of all the compounds, it can be observed that the halogen atoms are involved in interactions

View Article Online
DOI: 10.1039/C7DT03672H

with the methylene hydrogen atoms of the ligands, and this interaction is stronger in **1-Cl,2I$_3$** and **1-3Br$^-$I$_2$**. The distance between the *endo* H atom of the methylene bridge and the gold atom is 3.997, 2.592, 2.564 and 3.168 [3.405] Å respectively for **1-3PF$_6$**, **1-Cl,2I$_3$**, **1-3Br$^-$I$_2$** and **1-3I$_3$**. The H-C···X interaction angle is 140.08, 146.44, 160.39 and 154.73 [157.99]°, respectively. An ORTEP view of the distorted octahedral compounds in **1-Cl,2I$_3$**, **1-3Br$^-$I$_2$** and **1-3I$_3$** is reported in Figure 5. It is evident that in the case of **1-Cl,2I$_3$** and **1-3Br$^-$I$_2$**, the coordination plane AuC_4 and the segment X···Au···X are nearly orthogonal while in **1-3I$_3$** deviation from orthogonality is evident.

The crystal packing of the compounds is completed by I_3^- anions in the case of **1-Cl,2I$_3$**, I_2 molecules in the case of **1-3Br$^-$I$_2$** and acetonitrile solvent molecules in the case of **1-3I$_3$** (see Section 17 in the Supporting Information file).

Table 3: Selected bond distances (Å) and angles (deg) for cationic units in compounds **1-Cl,2I$_3$**, **1-3Br$^-$I$_2$** and **1-3I$_3$** compared with the analogous ones found in **1-3PF$_6$**. A diagram of the cationic complex is represented, together with a simplified labelling scheme.

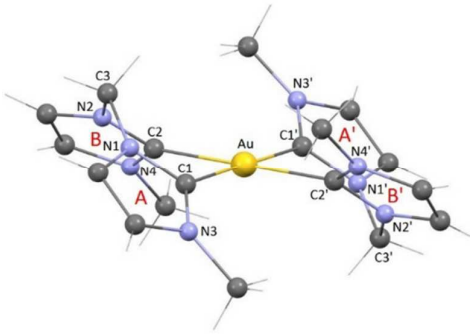

	1-3PF$_6$[a]	**1-Cl,2I$_3$**	**1-3Br$^-$I$_2$**	**1-3I$_3$**
Au-C1 [Au-C1′]	2.019(14) [2.075(15)]	2.049(9)	2.045(3)	2.046(9) [2.052(10)]
Au-C2 [Au-C2′]	2.046(13) 2.033(15)]	2.042(8)	2.045(3)	2.041(9) [2.045(10)]
C1-N1 [C1′-N1′]	1.337(19) 1.348(18)]	1.339(11)	1.344(4)	1.352(12) [1.348(13)]
C1-N3 [C1′-N3′]	1.367(17) [1.304(19)]	1.320(11)	1.358(4)	1.325(12) [1.348(13)]
C2-N2 [C2′-N2′]	1.345(17) [1.34(2)]	1.329(11)	1.344(4)	1.340(13) [1.352(13)]
C2-N4 [C2′-N4′]	1.360(17) [1.33(2)]	1.355(11)	1.358(4)	1.353(12) [1.332(12)]
C1-Au-C2 [C1′-Au-C2′]	83.5(5) [83.0(6)]	84.6(3)	83.50(19)	84.8(3) [84.9(4)]
C1-Au-C2′ [C2-Au-C1′]	97.0(5) [96.4(7)]	95.4(3)	96.50(19)	95.1(4) [95.2(4)]
AuC_4^A [AuC_4^A′]	43.44 [42.46]	41.47	39.53	40.38 [39.20]
AuC_4^B [AuC_4^B′]	42.32 [44.52]	41.07	39.53	40.24 [39.81]

a See reference 8.

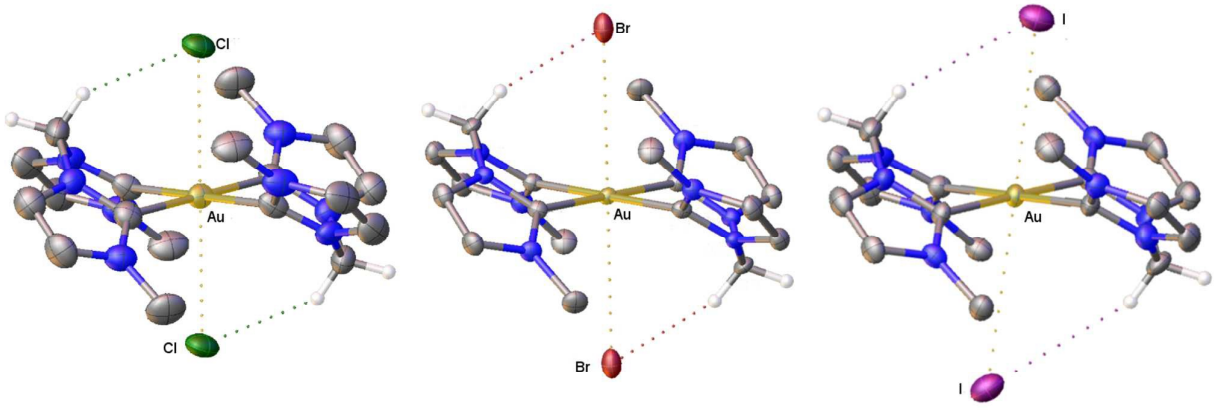

Figure 5. ORTEP views of compounds **1-Cl,2I$_3$** (left) **1-3Br$^-$I$_2$** (centre) and **1-3I$_3$** (right) evidencing the distorted octahedral coordination. Ellipsoids are shown at 50% probability level. Hydrogen atoms are omitted for clarity excepting *exo* and *endo* H atoms of the methylene bridge.

View Article Online
DOI: 10.1039/C7DT03672H

EXPERIMENTAL SECTION

General Remarks. All manipulations were carried out using standard Schlenk techniques under an atmosphere of argon or dinitrogen. The reagents were purchased by Aldrich as high-purity products and generally used as received; all solvents were used as received as technical grade solvents. The gold(III) complex $[Au(MeImCH_2ImMe)_2](PF_6)_3$ (**1-3PF$_6$**) was prepared according to literature procedures.[8] NMR spectra were recorded on a Bruker Avance 300 MHz (300.1 MHz for ^{1}H and 75.5 MHz for ^{13}C); chemical shifts (δ) are reported in units of parts per million (ppm) relative to the residual solvent signals. For the HRMS measurements, solutions of the complexes **1-3X** in DMSO at concentration of ca. 0.3 mM were injected at 10 µl/min by using a syringe pump. The HRMS measures were carried out with a Q-Exactive hybrid quadrupole-Orbitrap™ mass spectrometer (Thermo Fisher Scientific, Waltham, Massachusetts, USA). MS conditions were as followed: electrospray ionization in positive mode, resolution 70,000, AGC target $1\cdot10^6$, max injection time of 30 ms, scan range 150-2000 a.m.u, capillary voltage 3.5 kV and RF voltage at 50 V, capillary temperature 320°C and probe temperature 350°C; nitrogen was used as shealth gas at 11 psi. Calibration was performed with a standard solution purchased by Thermo Fisher Scientific (Pierce® ESI positive Ion Calibration Solution). The software for analysis of MS data was Xcalibur 3.1 (Thermo Fisher Scientific).

The identity of the compounds was determined by multinuclear NMR spectroscopy and HRMS spectrometry, considering that the CHN elemental analysis are slightly off because of residual water.

Synthesis of 1-3Cl. A solution of $Et_4NCl\cdot H_2O$ (0.5 mmol in 10 mL of CH_3CN) was slowly added to a solution of complex **1-3PF$_6$** (0.05 mmol) in CH_3CN (10 mL), leading immediately to the formation of a white precipitate. The reaction mixture was maintained under stirring for 1 hour and subsequently the product (white solid) was recovered by filtration, washed with Et_2O (3 mL) and finally dried under vacuum. White solid (yield 73%). Anal. Calcd for $C_{18}H_{34}AuCl_3N_8O_5$: C, 29.70; H, 4.43; N, 14.61%. Found: C, 28.54; H, 4.16; N, 15.08%. ^{1}H NMR (DMSO-d_6, 25 °C, ppm): δ = 3.65 (s, 12H, CH_3), 6.74 (d AB system, 2H, CH_2), 7.76 (s, 4H, CH), 7.87 (d AB system, 2H, CH_2), 8.00 (s, 4H, CH). ^{13}C NMR (DMSO-d_6, 25 °C, ppm): δ = 37.8 (CH_3), 62.8 (CH_2), 123.7 (CH), 125.0 (CH), 146.8 (NCN). MS (HRMS, base peak, *m/z*) = 274.0842 $[\mathbf{1}]^{2+}$ (required for $C_{18}H_{23}N_8Au^{2+}$= 274.0850), 292.0724 $[\mathbf{1Cl}]^{2+}$ (required for $C_{18}H_{24}N_8AuCl^{2+}$= 292.0733), 619.1144 $[\mathbf{1Cl_2}]^{+}$ (required for $C_{18}H_{24}N_8AuCl_2^{+}$= 619.1161).

Synthesis of 1-3Br. Same procedure described for **1-3Cl**, but using Et_4NBr. White solid (yield 73%). Anal. Calcd for $C_{18}H_{28}AuBr_3N_8O_2$: C, 26.20; H, 3.42; N, 13.58; Br, 29.05%. Found: C, 25.80; H, 3.49; N, 14.31; Br, 28.48%. ^{1}H NMR (DMSO-d_6, 25 °C, ppm): δ = 3.64 (s, 12H, CH_3), 6.78 (d AB system, 2H, CH_2), 7.68 (d AB system, 2H, CH_2), 7.77 (s, 4H, CH), 8.01 (s, 4H, CH). ^{13}C NMR (DMSO-d_6, 25 °C, ppm): δ = 38.3 (CH_3), 63.3 (CH_2), 123.9 (CH), 125.2 (CH), 146.1 (NCN). MS (HRMS, base peak, m/z) = 274.0833 $[\mathbf{1}]^{2+}$ (required for $C_{18}H_{23}N_8Au^{2+}$= 274.0850), 314.0462 $[\mathbf{1Br}]^{2+}$ (required for $C_{18}H_{24}N_8AuBr^{2+}$= 314.0481), 709.0091 $[\mathbf{1Br_2}]^{+}$ (required for $C_{18}H_{24}N_8AuBr_2^{+}$= 709.0131).

Synthesis of 1-3I. Same procedure described for **1-3Cl**, but using ^{n}Bu$_4$NI. White solid (yield 73%). Anal. Calcd for $C_{18}H_{26}AuI_3N_8O$: C, 22.80; H, 2.76; N, 11.81%. Found: C, 22.24; H, 2.71; N, 12.82%. ^{1}H NMR (DMSO-d_6, 25 °C, ppm): δ = 3.58 (s, 12H, CH_3), 6.81 (d AB system, 2H, CH_2), 7.29 (d AB system, 2H, CH_2), 7.78 (s, 4H, CH), 8.02 (s, 4H, CH). ^{13}C NMR (DMSO-d_6, 25 °C, ppm): δ = 39.6 (CH_3), 63.4 (CH_2), 124.3 (CH), 125.3 (CH), 145.8 (NCN). MS (HRMS, base peak, m/z) = 274.0840 $[\mathbf{1}]^{2+}$ (required for $C_{18}H_{23}N_8Au^{2+}$= 274.0850), 338.0403 $[\mathbf{1I}]^{2+}$ (required for $C_{18}H_{24}N_8AuI^{2+}$= 338.0412), 802.9845 $[\mathbf{1I_2}]^{+}$ (required for $C_{18}H_{24}N_8AuI_2^{+}$= 802.9873).

Crystallization of 1-3PF$_6$ with halide/iodine mixtures. Procedure for the Cl^-/I_2 sample. Acetonitrile solutions of **1-3PF$_6$** and $NaCl/I_2$ in an approximate concentrations 1:30:40 mM were prepared separately and then mixed. Crystals of **1-Cl,2I$_3$** suitable for X-ray analysis were obtained by slow diffusion of diethyl ether into this mixture. The same procedure was also applied for the mixtures KBr/I_2 and NaI/I_2, obtaining complexes **1-3Br$^-$I$_2$** and **1-3I$_3$** respectively.

Titration and Job Plot experiments. *Method A.* Solutions of **1-3PF$_6$** and of tetraalkylammonium halide were prepared in DMSO–d_6 (7.26 mM and 726 mM, respectively) or D_2O (0.42 mM and 42 mM). Increasing amounts of the halide solution have been added to the solution of the complex, and the resulting ^{1}H NMR spectrum was recorded at 25 °C. The variation on $\mathbf{1}^{3+}$ concentration at the end of the titration experiments was around -10% for the experiments in DMSO-d_6 and -20% for those in D_2O. *Method B.* In order to exclude the possibility that the observed variation of chemical shift was a consequence of aggregation/disaggregation of the complex in solution, some titrations at constant concentration of **1-3PF$_6$** were performed. A solution of complex **1-3PF$_6$** was prepared (1.25 ml, 7.26 mM in DMSO-d_6 or 0.42 mM in D_2O). An aliquot (0.40 ml) of this solution was then transferred in a second vial, where $Et_4NCl\cdot H_2O$ was added ($9.1\ 10^{-5}$ mol for the experiment in DMSO-d_6 and $1.05\ 10^{-4}$ mol for that in D_2O). The ^{1}H NMR titrations were then performed by sequential additions of this solution directly into the NMR tube containing the solution of the sole complex. The results perfectly matched those obtained with the first method, because the same speciation was obtained, and the stability constants differed by less than 0.1 log units.

For the Job Plot experiments two solutions of complex **1-3PF$_6$** (5 mM) and tetraalkylammonium halide (5 mM) in DMSO–d_6 were prepared. These solutions were mixed to give ten samples at different χ_X maintaining the $[\mathbf{1\text{-}3PF_6} + X^-]$ = 5mM. The ^{1}H NMR spectrum of every sample was recorded at 25 °C.

Calculation of stability constants and of the chemical shifts for the 1-halide complexes. The ^{1}H-NMR titrations and the job plots data (chemical shift vs. solution composition) were elaborated by the computer program PITMAP[13] to obtain the

View Article Online
DOI: 10.1039/C7DT03672H

stability constants (logβ) and the chemical shifts of each complex. The program calculates the theoretical value of Δd (*i.e.* the chemical shift difference between $\mathbf{1}^{3+}$ in the presence of the halide and $\mathbf{1}^{3+}$ alone) at each experimental point; for example, if the complexes $\mathbf{1X}^{2+}$ and $\mathbf{1X_2}^{+}$ form, the $\Delta\delta$ of CH_2 is given by the equation:

$$\Delta\delta = \Delta\delta_{CH_2(\mathbf{1X}^{2+})}\frac{[\mathbf{1X}^{2+}]}{C_{\mathbf{1}^{3+}}} + \Delta\delta_{CH_2(\mathbf{1X_2}^{+})}\frac{[\mathbf{1X_2}^{+}]}{C_{\mathbf{1}^{3+}}} \quad (3)$$

where $C_{\mathbf{1}^{3+}}$ is the total concentration of $\mathbf{1}^{3+}$ (experimentally known), and $\Delta\delta_{CH_2(\mathbf{1X}^{2+})}$ and $\Delta\delta_{CH_2(\mathbf{1X_2}^{+})}$ are the chemical shifts of CH_2 for each complex. Species concentration at equilibrium (e.g. [$\mathbf{1X}^{2+}$] and [$\mathbf{1X_2}^{+}$]) are calculated by solving the mass balance equations through the Newton–Raphson method.[27] Then, the sum of the squares of the differences between experimental and calculated chemical shift values are minimized using pitmapping[28] or simplex[27] as nonlinear least squares algorithms, by varying $\Delta\delta_{CH_2}$ (or $\Delta\delta_{CH_3}$) and logβ values of the complexes. Pitmapping method allows to compute also the standard deviation of the fitted parameters.

Computational details. Amsterdam Density Functional (ADF) software suite[29,30] was used to perform the density functional theory (DFT) calculations. Scalar relativistic effects were accounted for using the zeroth-order regular approximation (ZORA),[31] an optimal approach in presence of heavy nuclei.[32] The BLYP[33] density functional was chosen and the dispersion contribution term developed by Grimme *et al*.[34] (BLYP-D3(BJ)) was added. For all the elements we used the TZ2P basis set, which is a large uncontracted set of Slater-type orbitals (STOs), is of triple-ζ quality and was augmented with two sets of polarization functions on each atom (2p and 3d in the case of H, 3d and 4f in the case of C and N, 4d and 5f in the case of Cl, 5d and 6f in the case of Br, 6d and 7f in the case of I and 6g and 7h in the case of Au). Core electrons were treated with the frozen-core approximation: up to 1s for C and N, up to 2p for Cl, up to 3p for Br, up to 4p for I and up to 4d in the case of Au, respectively. The Becke grid was used for the numerical integration.[35] Symmetry constraints were imposed and are specified in the text. Solvent effects were taken into account with the Conductor-like Screening Model (COSMO),[36] as implemented in the ADF program. For DMSO and water we used a solvent-excluding surface with an effective radius of 3.04 and 1.93 Å, and relative dielectric constant of 46.7 and 78.39, respectively. The empirical parameter in the scaling function in the COSMO equation was set to 0.0. The radii of the atoms were taken to be MM3 radii,[37] divided by 1.2, giving 1.350 Å for H, 1.700 Å for C, 1.608 for N, 1.725 Å for Cl, 1.850 Å for Br, 1.967 Å for I and 2.025 Å for Au.[38]

In order to gain insight into the nature of the bonding between the gold complex and the halide ion(s), the activation strain model (ASM)[39] was employed, aiming at a meaningful description of structural and reactivity properties of the chemical species.[§] In this approach, the energy relative to the fragments forming the system, i.e. the gold complex and the halide ion(s), (ΔE), is decomposed into the strain contribution ΔE_{strain} and the interaction contribution ΔE_{int} (eq. 4):

$$\Delta E = \Delta E_{strain} + \Delta E_{int} \quad (4)$$

The activation strain ΔE_{strain} is the energy associated with deforming the fragments from their equilibrium geometry into the geometry they acquire when forming the complex of interest. It can be divided into a contribution stemming from each fragment. The interaction ΔE_{int} is the actual interaction energy between the deformed fragments. ΔE_{int} can be further analysed in the framework of the Kohn-Sham Molecular Orbital (MO) model using a quantitative energy decomposition analysis (EDA) of the bond into electrostatic attraction, Pauli repulsion (or exchange repulsion), and stabilizing orbital interactions (eq. 5).[39] Dispersion, which is included in our approach, must also be accounted for in the sum:

$$\Delta E_{int} = \Delta V_{elstat} + \Delta E_{Pauli} + \Delta E_{oi} + \Delta E_{disp} \quad (5)$$

Crystal data. Crystal data for complexes **1-Cl,2I$_3$** and **1-3I$_3$** were collected at room temperature on a Bruker APEX II single-crystal diffractometer, working with Mo-Kα graphite monochromatic radiator (λ = 0.71073 Å) and equipped with an area detector. The raw frame data (20 s per frame scan time for a sphere of diffraction data) were processed using SAINT software;[40] a correction for absorption was made using SCALE program[41] to yield the reflection data file, R(int) was 0.1821 before and 0.0950 after correction for compound **1-Cl,2I$_3$** and 0.1674 and 0.0661 for compound **1-3I$_3$**. The Ratio of minimum to maximum transmission is 0.2238 and 0.6603 respectively for the two complexes. The lambda/2 correction factor is 0.0015. Intensity data of compound **1-3Br$^-$I$_2$** were recorded at 100K at the Elettra Syncrothron Light Source facility (λ = 0.7000 Å) (CNR Trieste, Strada Statale 14, Area Science Park, 34149, Basovizza, Trieste, Italy). The raw frame data were processed using the program package CrysAlisPro 1.171.38.41.[42] R(int) was 0.1695 before and 0.0488 after correction. The Ratio of minimum to maximum transmission is 0.6768. The structures were solved by direct methods with SHELXS-97 and refined against F^2 with SHELXL-2014/7[43] using anisotropic thermal parameters for all non-hydrogen atoms. The hydrogen atoms were placed in the ideal geometrical positions. Details for the X-ray data collection are reported in Table S15. Crystallographic data for the complexes have been deposited with the Cambridge Crystallographic Data Centre as supplementary publications CCDC 1563831 (complex **1-Cl,2I$_3$**), 1563832 (complex **1-3Br$^-$I$_2$**), 1563833 (complex **1-3I$_3$**).

CONCLUSIONS

The $[Au(MeImCH_2ImMe)_2]^{3+}$ cation behaves as an anion receptor towards halides in DMSO and water. The stability constants for the gold-halides adducts are greater in DMSO following the order $Cl^- > Br^- > I^-$, whereas the order of selectivity is reversed in water. The good characteristics exhibited relay on: i) the high positive charge of the gold centre, ii) the proper square planar geometry which favours the anion approach, iii) the cooperative effect of the CH_2 and CH_3 groups, iv) the stacking of the cations which favours a

View Article Online
DOI: 10.1039/C7DT03672H

lipophilic micro-environment, v) the easy tunability of the dicarbene ligand. Most interestingly, the receptor system is thermally very stable and practically unaffected by pH changes in the 1-7 range. We are actually investigating the possibility of improving the sensitivity of the complex, by favouring the X···HC interaction (substitution of a methylene H with a more "expanded" CH_3 group) and by increasing its solubility in water, via introduction of PEG substituents in the imidazole fragments.[44]

Conflicts of interest

There are no conflicts to declare.

Acknowledgements

University of Padova is gratefully acknowledged for financial support (CPDA20140431 and *Assegno di Ricerca Senior* GRIC15V47A). Computational facilities at CINECA were available thanks to the ISCRA grant STREGA (PI: L.O.).

Notes and references

‡ The chemical shifts of the CH_2 group protons appears scarcely sensitive to the water content in DMSO. In fact, we obtained the same results in the titration experiments using $Et_4NCl{\cdot}H_2O$ and flask DMSO-d_6 or Et_4NCl and ampulla DMSO-d_6 in dry-box.

§ ΔG values should be rigorously considered, but since the entropic contribution is expected to be very similar in analogous compounds, trends based on electronic energies can be discussed with confidence.

§§ In order to verify this hypothesis, we have roughly added to the energy of the halides in gas-phase the experimental solvation energies of these ions in DMSO reported in ref. 23 and combined these results with the energies of the Au species relaxed in DMSO to calculate the reaction energies. For the formation on $\mathbf{1X^{2+}}$ we obtained -12.99, -8.22 and -8.17 kcal mol^{-1} in DMSO for Cl, Br and I, respectively; the values for the formation of $\mathbf{1X2^{+}}$ were -22.6, -13.45 and -13.43 kcal mol^{-1} in DMSO for Cl, Br and I, respectively. The trend were thus recovered. These preliminary observations suggest that the role of solvent deserves deeper scrutiny in combined novel experiments and computations.

1 See for example: (a) A. S. K. Hashmi, *Chem. Rev.*, 2007, **107**, 3180-3211. (b) N. Krause and C. Winter, *Chem. Rev.*, 2011, **111**, 1994–2009. (c) A. Corma, A. Leyva-Pérez and M. J. Sabater, *Chem. Rev.*, 2011, **111**, 1657–1712. (d) D.-A. Roşca, J. A. Wright and M. Bochmann, *Dalton Trans.*, 2015, **44**, 20785-20807. (e) R. Dorel and A. M. Echavarren, *Chem. Rev.*, 2015, **115**, 9028-9072. (f) M. Joost, A. Amgoune and D. Bourissou, *Angew. Chem. Int. Ed.*, 2015, **54**, 15022-15045.

2 R. Visbal and M. C. Gimeno, *Chem. Soc. Rev.*, 2014, **43**, 3551-3574.

3 (a) M. Monticelli, C. Tubaro, M. Baron, M. Basato, P. Sgarbossa, C. Graiff, G. Accorsi, T. P. Pell, D. J. D. Wilson and P. J. Barnard, *Dalton Trans.*, 2016, **45**, 9540-9552. (b) M. Baron, C. Tubaro, A. Biffis, M. Basato, C. Graiff, A. Poater, L. Cavallo, N. Armaroli and G. Accorsi, *Inorg. Chem.*, 2012, **51**, 1778-1784.

4 (a) R. Zhong, A. Pöthig, D. C. Mayer, C. Jandl, P. J. Altmann, W. A. Herrmann and F. E. Kühn, *Organometallics*, 2015, **34**, 2573–2579. (b) P. J. Altmann and A. Pöthig, *J. Am. Chem. Soc.*, 2016, **138**, 13171−13174. (c) F.-F. Hung, W.-P. To, J.-J. Zhang, C. Ma, W.-Y. Wong and C.-M. Che, *Chem. Eur. J.*, 2014, **20**, 8604–8614. (d) S. Kobialka, C. Müller-Tautges, M. T. S. Schmidt, G. Schnakenburg, O. Hollóczki, B. Kirchner and M. Engeser, *Inorg. Chem.*, 2015, **54**, 6100–6111.

5 (a) I. Ott, *Coord. Chem. Rev.*, 2009, **253**, 1670–1681. (b) T. Zou, C. T. Lum, C.-N. Lok, J.-J. Zhang, and C.-M. Che, *Chem. Soc. Rev.*, 2015, **44**, 8786-8801.

6 (a) M. Baron, C. Tubaro, M. Basato, A. Biffis, M. M. Natile and C. Graiff, *Organometallics*, 2011, **30**, 4607-4615. (b) M. Baron, C. Tubaro, M. Basato, A. Biffis and C. Graiff, *J. Organomet. Chem.*, 2012, **714**, 41-46. (c) M. Baron, C. Tubaro, M. Basato, A. A. Isse, A. Gennaro, L. Cavallo, C. Graiff, A. Dolmella, L. Falivene and L. Caporaso, *Chem. Eur. J.*, 2016, **22**, 10211-10224. (d) M. Baron, C. Tubaro, M. Basato, M. M. Natile and C. Graiff, *J. Organomet. Chem.*, 2013, **723**, 108-114.

7 (a) C.-Y. Wu, T. Horibe, C. Borch Jacobsen and F. D. Toste, *Nature*, 2015, 517, 449–454. (b) P. de Frémont, R. Singh, E. D. Stevens, J. L. Petersen and S. P. Nolan, *Organometallics*, 2007, **26**, 1376–1385. (c) M. Kriechbaum, D. Otte, M. List and U. Monkowius, *Dalton Trans.*, 2014, **43**, 8781-8791.

8 M. Baron, C. Tubaro, M. L. C. Cairoli, L. Orian, S. Bogialli, M. Basato, M. M. Natile and C. Graiff, *Organometallics*, 2017, **36**, 2285-2292.

9 A. H. Mageed, B. W. Skelton and M. V. Baker, *Dalton Trans.*, 2017, **46**, 7844-7856.

10 (a) P. Molina, F. Zapata and A. Caballero, *Chem. Rev.*, 2017, **117**, 9907−9972. (b) P. A. Gale, E. N. W. Howe and X. Wu, *Chem.*, 2016, **1**, 351-422. (c) M. L. Langton, C. J. Serpell and P. D. Beer, *Angew. Chem. Int. Ed.*, 2016, **55**, 1974-1987. (d) N. H. Evans and P. D. Beer, *Angew. Chem. Int. Ed.*, 2014, **53**, 11716-11754.

11 N. Busschaert, C. Caltagirone, W. Van Rossom and P. A. Gale, *Chem. Rev.*, 2015, **115**, 8038−8155.

12 (a) T. Zhang, L.-P. Zhou, X.-Q. Guo, L.-X. Cai and Q.-F. Sun, *Nat. Commun.*, 2017, **8**, 15898. (b) Q. Liu, X. Zhao, Z. Hu, Z. Zhao and H. Wang, *Sci. Rep.*, 2017, **7**, 7534. (c) A. S. McCall, H. Wang, J. M. Desper and S. Kraft, *J. Am. Chem. Soc.*, 2011, **133**, 1832–1848. (d) J. W. Steed, *Chem. Soc. Rev.*, 2009, **38**, 506-519. (e) P. J. Altmann and A. Pöthig, *Chem. Commun.*, 2016, **52**, 9089-9092. (f) A. M. J. Devoille, P. Richardson, N. L. Bill, J. L. Sessler and J. B. Love, *Inorg. Chem.*, 2011, **50**, 3116-3126.

13 V. B. Di Marco, PhD Thesis, University of Padova, 1998.

14 (a) L. M. Eytel, A. K. Gilbert, P. Görner, L. N. Zakharov, D. W. Johnson and M. M. Haley, *Chem. Eur. J.*, 2017, **23**, 4051-4054. (b) L. A. Jowett, E. N. W. Howe, V. Soto-Cerrato, W. Van Rossom, R. Pérez-Tomás and P. A. Gale, *Sci. Rep.*, 2017, **7**, 9397.

15 R. Kumar, S. Sandhu, P. Singh and S. Kumar, *Chem. Rec.*, 2017, **17**, 441-471.

16 (a) S. Ruiz-Botella, P. Vidossich, G. Ujaque and E. Peris, *Chem. Eur. J.*, 2016, **22**, 15800-15806. (b) S. Ruiz-Botella, P. Vidossich, G. Ujaque, E. Peris and P. D. Beer, *RSC Adv.*, 2017, **7**, 11253-11258. (c) C.-L. Do-Thanh, N. Khanal, Z. Lu, S. A. Cramer, D. M. Jenkins and M. D. Best, *Tetrahedron*, 2012, **68**, 1669-1673.

17 X. Jiang, M. Feng, D. Zhang, B. Wang, Z. Dong and G. Gao, *Chin. J. Chem.*, 2013, **31**, 673-678.

18 M. J. Chmielewski, M. Charon and J. Jurczak, *Org. Lett.*, 2004, **6**, 3501-3504.

19 S. O. Kang, J. M. Llinares, D. Powell, D. WanderWelde and K. Bowman-James, *J. Am. Chem. Soc.*, 2003, **125**, 10152-10153.

20 (a) M. J. Langton, I. Marques, S. W. Robinson, V. Félix and P. D. Beer, *Chem. Eur. J.,* 2016, **22**, 185-192. (b) R. A. Bilbeisi, T. Prakasam, M. Lusi, R. El Khoury, C. Platas-Iglesias, L. J.

View Article Online
DOI: 10.1039/C7DT03672H

Charbonnière, J.-C. Olsen, M. Elhabiri and A. Trabolsi, *Chem. Sci.*, 2016, **7**, 2524-2531.
21 L. Orian, P. Ganis, S. Santi and A. Ceccon, *J. Organomet. Chem.*, 2005, **690**, 482-492.
22 M. D. Đurović, R. Puchta, Ž. D. Bugarčić and R. van Eldik, *Dalton Trans.*, 2014, **43**, 8620-8632.
23 Y. J. Marcus, *Chem. Soc., Faraday Trans.*, 1991, **87**, 2995-2999.
24 H. Haller and S. Riedel, *Z. Anorg. Allg. Chem.*, 2014, **640**, 1281-1291.
25 Z. Lu, S. A. Cramer and D. M. Jenkins, *Chem. Sci.*, 2012, **3**, 3081-3087.
26 S. Alvarez, *Dalton Trans.*, 2013, **42**, 8617-8636.
27 W. H. Press, B. P. Flannery, S. A. Teukolsky and W. T. Vetterling, *Numerical Recipes: The Art of Scientific Computing*, Cambridge University Press, Cambridge, 1986.
28 L. G. Sillén, *Acta Chem. Scand.*, 1964, **18**, 1085-1098.
29 E. J. Baerends, D. E. Ellis and P. Ros, *Chem. Phys.*, 1973, **2**, 41-51.
30 (a) G. te Velde, F. M. Bickelhaupt, E. J. Baerends, C. Fonseca Guerra, S. J. A. van Gisbergen, J. G. Snijders and T. Ziegler, *J. Comput. Chem.*, 2001, **22**, 931-967. (b) Computer code ADF2014 E. J. Baerends, et al. (SCM, Theoretical Chemistry, Vrije Universiteit, Amsterdam, The Netherlands, 2014).
31 E. van Lenthe, E. J. Baerends and J. G. Snijders, *J. Chem. Phys.*, 1994, **101**, 9783-9792.
32 (a) F. Zaccaria, L. P. Wolters, C. Fonseca Guerra and L. Orian, *J. Comp. Chem.*, 2016, **37**, 1672-1680. (b) S. Scuppa, L. Orian, A. Donoli, S. Santi and M. Meneghetti, *J. Phys. Chem. A,* 2011, **115**, 8344-8349. (c) S. Santi, C. Durante, A. Donoli, A. Bisello, L. Orian, P. Ganis, A. Ceccon and F. Benetollo, *Organometallics,* 2010, **29**, 2046-2053. (d) L. Orian, W.-J. van Zeist and F. M. Bickelhaupt, *Organometallics*, 2008, **27**, 4028-4030.
33 (a) A. D. Becke, *Phys. Rev. A*, 1988, **38**, 3098-3100. (b) C. Lee, W. Yang and R. G. Parr, *Phys. Rev. B*, 1988, **37**, 785-789.
34 S. Grimme, S. Ehrlich and L. Goerigk, *J. Comp. Chem.*, 2011, **32**, 1456-1465.
35 (a) A. D. Becke, *J. Chem. Phys.*, 1988, **88**, 2547-2553. (b) M. Franchini, P. H. T. Philipsen and L. Visscher, *J. Comput. Chem.*, 2013, **34**, 1819-1827.
36 (a) A. Klamt and G. J. Schürmann, *Chem. Soc., Perkin Trans. 2*, 1993, **5**, 799-805. (b) A. Klamt, *J. Phys. Chem.*, 1995, **99**, 2224-2235.
37 C. C. Pye and T. Ziegler, *Theor. Chem. Acc.*, 1999, **101**, 396-408.
38 N. L. Allinger, X. Zhou and J. Bergsma, *J. Mol. Struct. (Theochem)*, 1994, **312**, 69-83.
39 F. M. Bickelhaupt and E. J. Baerends, Kohn-Sham Density Functional Theory: Predicting and Understanding Chemistry. In Reviews in Computational Chemistry; John Wiley & Sons, Inc., 2007, 1-86.
40 SAINT, Version 7.06a; Bruker AXS Inc.: Madison, Wisconsin, USA.
41 G. M. Sheldrick, SADABS 2000 Version 2.01, Bruker AXS Inc., Madison, Wisconsin, USA.
42 CrysAlisPro 1.171.38.41 (Rigaku Oxford Diffraction, 2015).
43 (a) G. M. Sheldrick, 1998, SHELX97, Version Release 97-2, University of Göttingen, Germany. (b) G. M. Sheldrick, *Acta Cryst.,* 2008, **A64**, 112.
44 M. Baron, S. Bellemin-Laponnaz, C. Tubaro, M. Basato, S. Bogialli and A. Dolmella, *J. Inorg. Biochem.*, 2014, **141**, 94-102.

View Article Online
DOI: 10.1039/C7DT03672H

Efficient gold(III) based halides receptor via cooperative Au···X and X···HC interactions

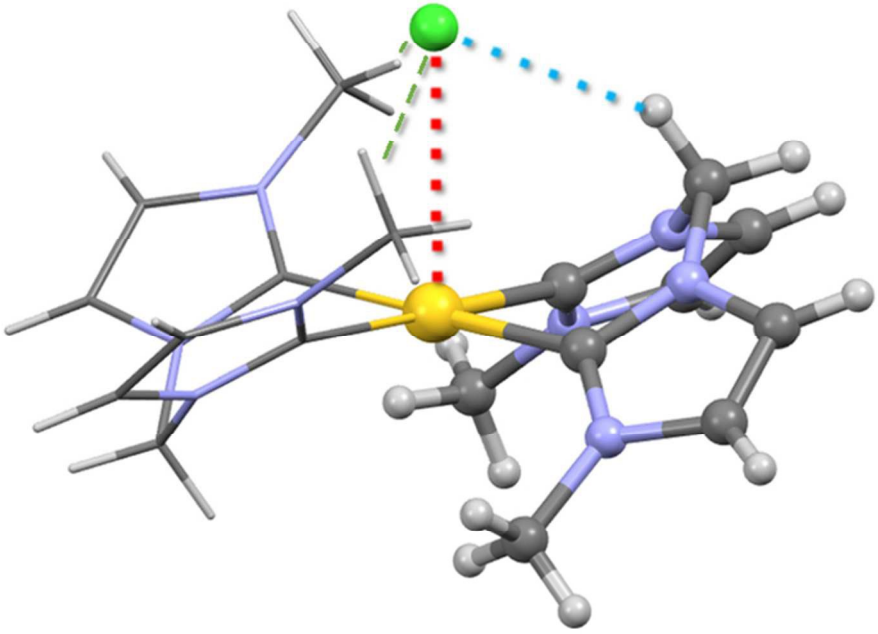

69x61mm (300 x 300 DPI)